Bistability and all-optical switching in semiconductor ring lasers

Toni Pérez[1], Alessandro Scirè[1] , Guy Van der Sande[1,2], Pere Colet[1] and Claudio R. Mirasso[1]

[1]*Instituto de Física Interdisciplinar y Sistemas Complejos, IFISC, UIB-CSIC, E-07122 Palma de Mallorca, Spain*

[2]*Department of Applied Physics and Photonics, Vrije Universiteit Brussel, Pleinlaan 2, 1050 Brussels, Belgium*

scire@ifisc.uib.es

Abstract: Semiconductor ring lasers display a variety of dynamical regimes originating from the nonlinear competition between the clockwise and counter-clockwise propagating modes. In particular, for large pumping the system has a bistable regime in which two stationary quasi-unidirectional counter-propagating modes coexist. Bistability is induced by cross-gain saturation of the two counter-propagating modes being stronger than the self-saturation and can be used for data storage when the semiconductor ring laser is addressed with an optical pulse. In this work we study the response time when an optical pulse is injected in order to make the system switch from one mode to the counter-propagating one. We also determine the optimal pulse energy to induce switching.

© 2007 Optical Society of America

OCIS codes: (140.3560) Lasers, ring; (140.5960) Semiconductor lasers; (200.4660) Optical logic

References and links

1. C. O. Weiss and R. Vilaseca, "Dynamics of lasers," Weinheim, New York (1991), and refs therein.
2. Q. L. Williams, and R. Roy, "Fast polarization dynamics of an erbium-doped fiber ring laser," Opt. Lett, **21**, 1478 (1996).
3. H. Nakatsuka, S. Asaka, H. Itoh, K. Ikeda, and M. Matsuoka, "Observation of bifurcation to chaos in an all-optical bistable system ," Phys. Rev. Lett, **50**, 109 (1983)
4. E. J. D'Angelo, E. Izaguirre, G. B. Mindlin, L. Gil, and J. R. Tredicce, "Spatiotemporal dynamics of lasers in the presence of an imperfect O(2) symmetry," Phys. Rev. Lett, **68**, 3702 (1992).
5. W. W. Chow, J. Gea-Banacloche, L. M. Pedrotti, V. E. Sanders, W. Schleich and M. O. Scully, "The ring laser gyro," Rev. Mod. Phys. **57** 61 (1985).
6. T. Krauss, P. J. R. Laybourn and J. S. Roberts, "CW operation of semiconductor ring lasers," Electron. Lett. **26**, 2095 (1990).
7. M. Sorel, J. P. R. Laybourn, A. Scirè, S. Balle, G. Giuliani, R. Miglierina,S. Donati, "Alternate oscillations in semiconductor ring lasers," Opt. Lett. **27**, 1992 (2002).
8. M. Sorel, G. Giuliani,A. Scirè, R. Miglierina, J. P. R. Laybourn, S. Donati, "Operating regimes of GaAs-AlGaAs semiconductor ring lasers: experiment and model," IEEE J. Quantum Electron. **39**, 1187 (2003).
9. J. J. Liang, S. T. Lau, M. H. Leary and J. M. Ballantyne, "Unidirectional operation of waveguide diode ring lasers," Applied Phys. Lett. **70**, 1192 (1997).
10. S.Zhang, Y. Liu, D.Lenstra, M.T.Hill, H.Ju, G.D. Khoe, H.J.S.Dorre, "Ring-laser optical flip-flop memory with single active element," J. Sel. Top. Q. Electron. **10**, 1093 (2004).
11. V. R. Almeida, C. A. Barrios, R. P. Panepucci, M. Lipson, M. A. Foster, D. G. Ouzounov, A. L. Gaeta, "All-optical switching on a silicon chip," Opt. Lett. **29**, 2867 (2004).
12. V. R. Almeida and M. Lipson, "Optical bistability on a silicon chip," Opt. Lett. **29**, 2387 (2004).

#82978 - $15.00 USD Received 11 May 2007; revised 31 Jul 2007; accepted 1 Aug 2007; published 24 Sep 2007

13. M. T. Hill, H. J. S. Dorren, T. de Vries, X. J. M. Leijtens, J. H. den Besten, B. Smalbrugge,Y. S Oei, H. Binsma, G. D. Khoe, M. K. Smit, "A fast low-power optical memory based on coupled micro-ring lasers," Nature **432**, 206 (2004).
14. G. H. M. van Tartwijk, D. Lenstra, "Semiconductor lasers with optical injection and feedback," Quantum Semiclass. Opt. **7**, 87 (1995).
15. V. Annovazzi-Lodi, A. Scirè, M. Sorel, S. Donati, "Dynamic behavior and locking of a semiconductor laser subjected to external injection," IEEE J. Quantum Electron. **34**, 2350 (1998).
16. M. San Miguel, R. Toral, "Stochastic Effects in Physical Systems," Instabilities and Nonequilibrium Structures V, edited by Tirapegui E., Martinez J., and Tiermann R., Netherlands: Kluwer Academic Publishers, (1999).

1. Introduction

Ring lasers have been the subject of a large amount of experimental and theoretical investigations [1], ranging from fundamental studies of their non-linear dynamics [2, 3, 4], to practical applications as the ring laser gyroscope [5]. Recently, circular Semiconductor Ring Lasers (SRLs) have been investigated due to their peculiar two-mode dynamical properties arising from the nonlinear interaction between the clockwise (CW) and counter-clockwise (CCW) propagating modes [6]. For practical applications it is necessary to be able to extract the light from the system which can be done using for example a y-junction output coupler [7]. The output coupler itself induces further interaction between the two counter-propagating modes. Therefore, to properly model the dynamics of this system, it is necessary to take this backscattering into account. A suitable dynamical model was introduced in Ref. [8] and its parameters were carefully fitted from the experimental results. Close to the laser threshold both modes coexist with the same stationary power. Increasing the pump, the system enters in oscillatory regime in which the intensity of both modes oscillates in antiphase. Finally for larger pumps the system enters in a bistable regime in which two stationary quasi-unidirectional counterpropagating modes coexist [8]. Bistable operation has been demonstrated in several structures beyond circular SRL [8], such as triangular SRL [9], double SRL sharing the same active element [10], and passive silicon rings [11, 12]. Recently, the study of bistability in a tandem of two SRLs [13] unveiled highly appealing features for applications in all-optical switching and optical memories.

However, while most of the previous studies have focused on the characterization of the stationary states of the system there is a lack of studies about the transient response of SRL when it is addressed with an optical pulse. Therefore, little is known about the intensity or the duration required for the pulse in order to induce a successful switching. Neither the time it takes the system to switch from one mode to the counterpropagating one has been characterized. These issues are extremely relevant for the envisioned applications.

In this work we study the response of a SRL operating in the bistable regime when a coherent optical pulse is injected in order to induce a switch from one of the quasi-unidirectional mode to the counter-propagating one. We include the presence of spontaneous emission noise in our modeling. We perform a statistical analysis of the time it takes the system to start emitting in the other mode after the pulse has been applied (switching time). We also analyze the energy the pulse should have in order to induce switching. Furthermore, pulses of several shapes are considered to elucidate that, in order to induce switching, the relevant characteristic of the pulse is its integrated energy rather than its amplitude or duration.

2. Model

The theoretical analysis of the two-mode ring laser is based on a set of dimensionless semiclassical Lamb equations for the two (slowly varying) complex amplitudes of the counterpropagating fields E_1 Clockwise (CW mode) and E_2 Counter Clockwise (CCW mode), which has provided a good quantitative description of the two-mode dynamics in SRLs [7, 8]. The

#82978 - $15.00 USD Received 11 May 2007; revised 31 Jul 2007; accepted 1 Aug 2007; published 24 Sep 2007
(C) 2007 OSA

equations read:

$$\dot{E}_{1,2} = \frac{(1+i\alpha)}{2}\left[N(1-s|E_{1,2}|^2 - c|E_{2,1}|^2) - 1\right]E_{1,2} \\ -(k_d + ik_c)E_{2,1} + \frac{\tau_p}{\tau_{in}}F_{1,2}(t) + \sqrt{\beta\,\tau_p N}\,\zeta_{1,2}(t) \quad (1)$$

where α accounts for phase-amplitude coupling and the self and cross saturation coefficients are given by s and c, respectively; the parameters k_d and k_c represent the dissipative and conservative components of the backscattered field, respectively. The term $F_{1,2}(t)$ represents resonant (zero-detuning) optical injection in the two modes, and it will be used to trigger the switching. Formally, this term is introduced according to the standard theory of injection in semiconductor

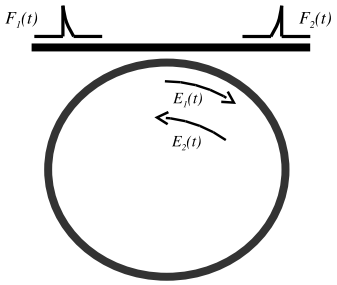

Fig. 1. Geometry of the SRL device and the injection scheme.

laser [14, 15], τ_p is the photon lifetime and τ_{in} the flight time in the ring cavity. The practical implementation of the optical injection is sketched in Fig. 1. The last term of Eq.(1) represents spontaneous emission noise; $\beta = 5\cdot 10^{-3}$ ns^{-1} represents the fraction of the spontaneously emitted photons coupled to mode 1 or 2. $\zeta_{1,2}$ are two independent complex Gaussian random numbers, with zero mean $\langle\zeta_i(t)\rangle = 0$ and correlation $\langle\zeta_i(t)\zeta_j^*(t')\rangle = 2\delta_{ij}\delta(t-t')$. The carrier density N obeys the rate equation for semiconductor lasers,

$$\dot{N} = \gamma\left[\mu - N - N(1-s|E_1|^2 - c|E_2|^2)|E_1|^2 - N(1-s|E_2|^2 - c|E_1|^2)|E_2|^2\right] \quad (2)$$

where μ is the dimensionless pump ($\mu \sim 1$ at laser threshold). In the set (1)-(2) the dimensionless time is rescaled by the photon lifetime τ_p. The parameter γ is the ratio of τ_p over the carrier lifetime τ_s.

3. Steady state solution and bistability

In order to perform a steady state analysis, we study the set of Eq. (1)-(2) without the optical injection and spontaneous emission terms. The equation (1) becomes:

$$\dot{E}_{1,2} = \frac{(1+i\alpha)}{2}\left[N(1-s|E_{1,2}|^2 - c|E_{2,1}|^2) - 1\right]E_{1,2} - (k_d + ik_c)E_{2,1} \quad (3)$$

We consider a SRL with 2-μm-wide single-transverse-mode ridge waveguides in a double-quantum-well GaAs/AlGaAs structure with 1-mm ring radius. The estimated parameter values for this device are [7]: $\alpha = 3.5$, $s = 0.005$, $c = 0.01$, $k_c = 0.0044$, $k_d = 0.000327$, $\gamma = 0.002$, $\tau_p = 10$ ps and $\tau_{in} = 0.6$ ps.

The stationary solutions of the set (2)-(3) can be expressed in the form $E_{1,2} = Q_{1,2}\exp(i\omega t + i\phi_{1,2})$, and the corresponding value for N. Fig. 2 shows the bifurcation dia-

#82978 - $15.00 USD Received 11 May 2007; revised 31 Jul 2007; accepted 1 Aug 2007; published 24 Sep 2007
(C) 2007 OSA

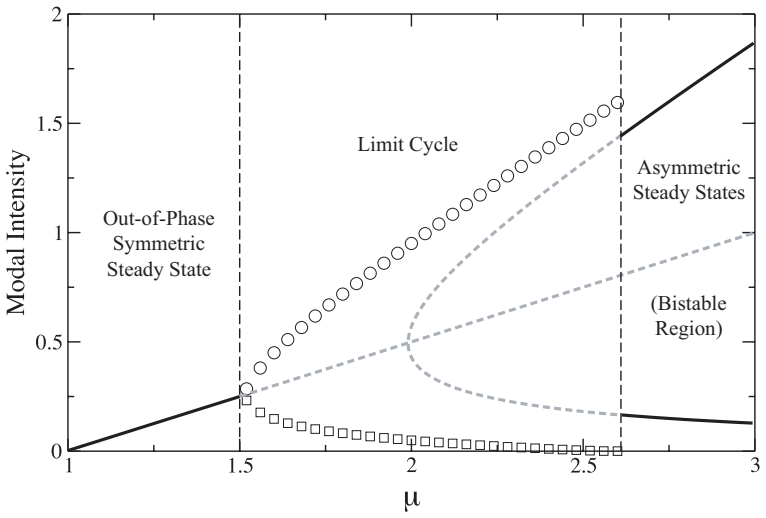

Fig. 2. Bifurcation diagram for the field intensities $Q^2_{1,2}(t)$. Symbols indicate the extrema of the field intensities in the oscillatory regime: open circle (square) represent the maxima (minima) of both $Q^2_1(t)$ and $Q^2_2(t)$. The stable steady states are denoted by thick black lines, and unstable steady states by grey dashed lines.

gram for the parameters considered here. At $\mu \sim 1$ laser oscillation takes place. The presence of dissipative backscattering (k_d) favors the presence of two steady state symmetric solutions ($Q_1 = Q_2 = Q$) just above threshold, despite the presence of strong cross-saturation between the two modes [7]. These two symmetric steady states have the same field amplitude and carrier inversion:

$$Q^2 = \frac{N-1+k_d}{(c+s)N} \tag{4}$$

$$N = \frac{\mu}{1+2Q^2-2(c+s)Q^4} \tag{5}$$

but they differ in the relative phase between the CW and CCW modes ($\Phi = \phi_2 - \phi_1$). The In-Phase Symmetric Solution (IPSS) corresponds to $\Phi = 0$ while the Out-of-Phase Symmetric Solution (OPSS) corresponds to $\Phi = \pi$. Since we are considering a positive value of k_d, the OPSS is the stable symmetric solution. The OPSS solution exists for any value of the pump above the threshold. However, it is not always stable. In Fig. 2 we have plotted the OPSS with a solid black line from the laser threshold to $\mu \sim 1.5$. At this current the OPSS is destabilized to a Hopf bifurcation. We have indicated the unstable OPSS with a straight grey dashed line. The Hopf bifurcation leads to the emergence of a oscillatory behavior in which the CW and the CCW modes coexist. The intensity of both modes oscillate with the same amplitude but are in antiphase. The oscillations are driven by the conservative part of the back-scattering coefficient k_c, and represent a dynamic competition between the two counterpropagating modes. We have determined the limit cycle from numerical integration of Eq. (2)-(3). We represent the maxima (minima) of the oscillating modal intensities by open circles (squares). This oscillatory behavior is stable up to $\mu \sim 2.6$.

We now turn back to the OPSS solution, which although it is unstable its further bifurcations are important for the behavior at large pump values. At $\mu \sim 2.0$, two unstable asymmetric solutions emerge at a pitchfork bifurcation from the unstable OPSS and they coexist with the stable limit cycle. We have obtained the asymmetric steady states by solving the right hand sides of

#82978 - $15.00 USD Received 11 May 2007; revised 31 Jul 2007; accepted 1 Aug 2007; published 24 Sep 2007
(C) 2007 OSA

Eq. (2)-(3) equated to zero with a Newton-Raphson method. These two stationary states consist in laser emission mainly concentrated in one propagation direction, i.e. quasi Clockwise (qCW) or quasi Counterclockwise (qCCW). In the qCW steady state the CW intensity takes a value on the upper branch while the CCW intensity takes a value in the lower branch. The qCCW steady state corresponds to the opposite situation. The contrast factor between the two modes $C = \frac{|E_1|^2-|E_2|^2}{|E_1|^2+|E_2|^2}$ increases with μ from the pitchfork bifurcation. Because the asymmetric stationary states are initially unstable, we have plotted them with grey dashed lines from $\mu \sim 2.0$ up to $\mu \sim 2.6$. At this current value the stable limit cycle loses its stability and the asymmetric stationary solution becomes stable (denoted as solid lines). For high pump values, the strong cross-saturation between the two counterpropagating waves tends to favor the quasi-unidirectional behavior. In this regime the device shows bistability between the two asymmetric solutions, and we refer to it as the *bistable regime*. This bistability between counterpropagating modes can be used for data storage when the SRL is addressed with an optical pulse. In the next section, we quantify the speed of and the necessary pulse energy to achieve successful data storage. We should note that as the cross-saturation parameter c tends to s the pitchfork bifurcation moves towards infinite pumping values. Therefore, a large cross-saturation value is required to have bistability.

4. Switching

In the bistable regime, if no injection is applied, the system relaxes to one of the two counterpropagating quasi-unidirectional stable states (qCW and qCCW) discussed in the previous section. Applying a pulse whose propagation direction is the opposite to the one of the dominating mode, it is possible to induce a switching from the original steady state to the other one. We chose as an optical trigger a pulse of the form $F_{1,2} = A\exp(-t/\tau)$, characterized by the pulse amplitude A, and the pulse decay time τ. The trigger amplitude A is in general complex, due to the (constant) dephasing accumulated by the external field in the optical wave guide outside the laser cavity. However, it is known that such associated phase does not affect the injection properties [15], and we assume A to be real.

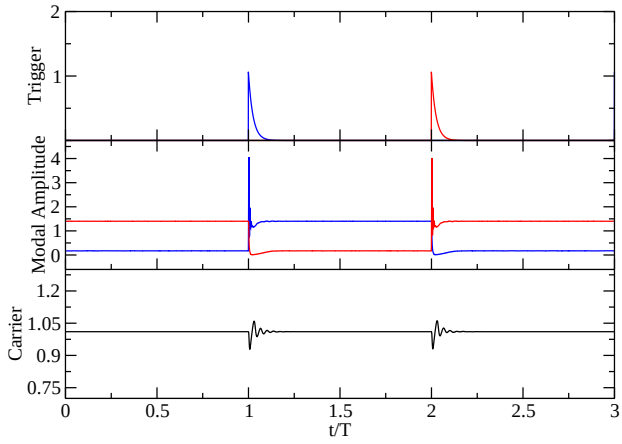

Fig. 3. Time traces of the dynamic variables under pulsed optical injection operation conditions. Upper panel: dimensionless trigger amplitude $|F_1(t)|$ (blue), and $|F_2(t)|$ (red). Middle panel: dimensionless SRL modal amplitudes $|E_1(t)|$ (blue), and $|E_2(t)|$ (red). Lower panel: carrier. The trigger characteristics: $A = 0.1$, $\tau = 0.1\,T$, $T = 10$ ns. $\mu = 3.0$, corresponding to $C \sim 0.85$.

#82978 - $15.00 USD Received 11 May 2007; revised 31 Jul 2007; accepted 1 Aug 2007; published 24 Sep 2007
(C) 2007 OSA

We have numerically integrated Eqs (1)-(2) through the second order Heun algorithm [16]. The optical injection was a stream of 1000 trigger pulses (alternating the CW and CCW) at a constant rate of 0.1 GHz to generate the statistics. Numerical simulation (see Fig. 3) show that if the system is in the qCW (qCCW) state and a CCW (CW) pulse is applied, a switching occurs to the qCCW (qCW) state if the switching energy exceeds a critical amount. The carriers show relaxation oscillations which are triggered by the pulse. In the regime we are operating these oscillations, which damp with a time constant of ~ 1 ns, die at the end of the pulse. However, for very short trigger pulses ($\tau/T < 0.01$) the oscillations may persist after the pulse ends ($\sim$ 1.5 ns). When a pulse is applied the response of the system is very fast. This allows for high speed optical data storage. However, please note that the time the system takes to reach the steady state after the switching event is longer than the response or switching time. This will limit the time between consecutive successful switching events. In this work, we concentrate only on characterizing the switching event.

We have computed the mean normalized cross-correlation between $P_1 = |E_1|^2$ and $P_2 = |E_2|^2$, evaluated at a time delay equal to the trigger period T, that is

$$X(T) = \frac{1}{\bar{P_1}\bar{P_2}} \frac{1}{T_{max}} \int_0^{T_{max}} P_1(t) P_2(t-T) dt \tag{6}$$

where $T_{max} = 1000\,T$ is the total integration time, $\bar{P_1} \sim \mu - 1$ is the average values of the intensity $|\bar{E_1}|^2$ when the (solitary) qCW mode is active (the same holds for the CCW mode intensity $\bar{P_2}$). Note that the normalization procedure that we use allows $X(T)$ to be slightly larger than one, due to the power injected by the trigger. If all the trigger pulses induce a switching $X(T) \sim 1$, whereas if some switching events fail $X(T)$ decreases and approaches to zero if no switchings occur. We have computed the value of $X(T)$ for different values of the trigger amplitude and decay time, and the result is shown in Fig. 4. The numerical simulations show that the shape of the pulse is not critical for the switching to occur, being the relevant magnitude its energy, given by $\varepsilon = \int_0^\infty |F_{1,2}|^2 dt = A^2\,\tau/2$. Figure 4 shows that a transition to

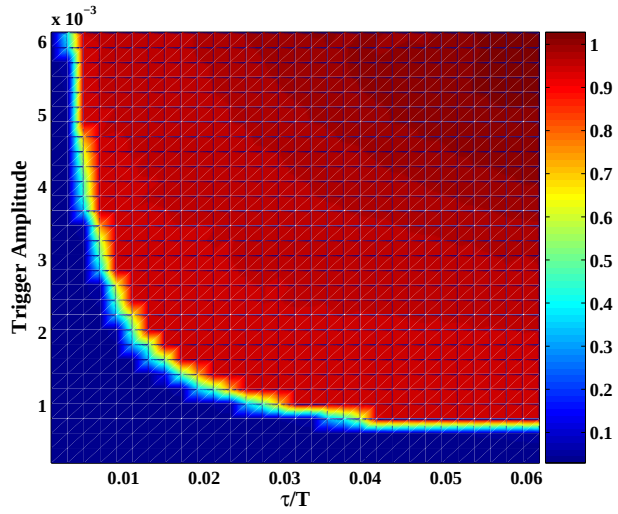

Fig. 4. Cross-correlation function $X(T)$, given by Eq. (6), versus the dimensionless trigger amplitude A and the pulse decay time τ normalized to the pulse repetition rate $T = 10$ ns. Parameters as in Fig. 3. Colorbar indicates values of the cross-correlation function.

successful switching events occurs in correspondence of an iso-energy curve for the trigger

#82978 - $15.00 USD Received 11 May 2007; revised 31 Jul 2007; accepted 1 Aug 2007; published 24 Sep 2007
(C) 2007 OSA

pulse, corresponding to a minimum (critical) switching energy $\varepsilon_c \sim 10fJ$, which has been calculated assuming 100 mW of optical power inside the cavity, in agreement with the output optical power and coupler efficiency measured in real devices. With the same data, and after each pulse is applied, we calculate the time it takes the system to reach one half of the value of the intensity of the final state ($\overline{P}_{1,2}$). This time (t_R from now on) is an estimation of the response time of the system to the trigger pulse, and characterizes the switching speed (see Fig. 5). Due to the presence of noise, t_R undergoes a statistic distribution, that we characterize through its mean value $< t_R >$ and variance $\sigma_R = \sqrt{< t_R^2 > - < t_R >^2}$ for different values of the trigger energy. From Fig. 5 we can determine the optimal energy of the optical pulse. For pulses with energies lower than 5 fJ the response time diverges, so one should avoid using such pulses. Increasing the energy of the pulse beyond 5 fJ produces a very limited decrease of the switching time, so there is little advantage in using stronger pulses. Therefore the optimal energy of the pulse seems to be around 5 fJ. At this optimal point the switching time is found to be below 100 ps. This result is practically independent of the trigger shape. The values of the error bars, corresponding to σ_R, are comprised inside the symbol sizes which indicates that, for the parameter we have considered, the fluctuations in the switching time are very small. The

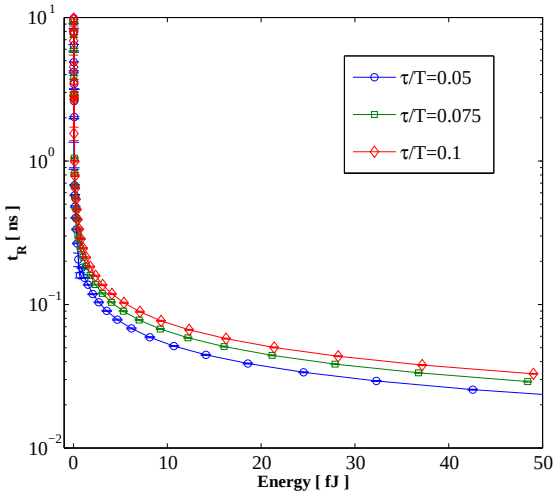

Fig. 5. Statistics of the response time t_R vs dimensionless trigger pulse amplitude A. dots: mean value $< t_R >$; error bars $\sigma_R = \sqrt{< t_R^2 > - < t_R >^2}$ for different τ/T. Parameters as in Fig. 3.

obtained response time is throughout much shorter than the inverse of the relaxation oscillation frequency ($\tau_{rel.ox} = f_{rel.ox}^{-1}$, where $f_{rel.ox} = \frac{1}{2\pi\tau_p}\sqrt{\gamma(\mu-1)} \sim 1GHz$) for our parameter values. This accounts for the fact that the switching itself represents an energy redistribution between the two states of the electric field, where field-medium energy exchange processes do not come significantly into play during the switching.

5. Conclusion

In conclusion, we have theoretically investigated the emergence of a bistable regime in a two-mode model for a SRL. The bistability takes place between two counter-propagating quasi-unidirectional solutions for the electric field, which well above threshold are stable solutions

#82978 - $15.00 USD Received 11 May 2007; revised 31 Jul 2007; accepted 1 Aug 2007; published 24 Sep 2007
(C) 2007 OSA

due to the cross-saturation mechanism in the gain. In this bistable regime we have analyzed the switching from one quasi-unidirectional solution to the counter-propagating one induced by the injection of a coherent optical pulse, in view of the possible implementation of a single SRL as an optically addressable memory element. We have found that the switching time of the system depends mainly on the energy of the pulse rather than on its amplitude or duration. For pulses of energy around 5 fJ the switching time is below 100 ps. It turns out that pulses of this energy are about optimal in the sense that the switching time diverges for weaker pulses and there is limited advantage in using stronger pulses (for 50 fJ pulses the switching time reduces to about 20 ps). These values are robust against spontaneous emission noise and rather insensitive to the trigger shape (e.g. we have obtained similar results for square or gaussian pulses). These values are expected to scale down with the device radius, due to the consequent decreasing of the cavity flight time. In principle, faster (*ps* or sub-*ps*) time scales would require more sophisticated (e.g. traveling-wave) modeling approach, and will be the subject of future investigations.

Acknowledgments

This work has been funded by the Spanish MEC and Feder under project TEC2006-10009/MIC (Conoce 2) and FIS2004-00953 (PhoDeCC), by the European Community under projects IST-2005-34743 (IOLOS) and IST-2005-34551 (PICASSO), and by the Balear Government under project PROGECIB-5A (QULMI). T.P. acknowledges support from the Govern Balear (Spain). A.S. acknowledges Ramon y Cajal program by MEC G.V. is a Postdoctoral Fellow of the Research Foundation - Flanders (FWO). The authors wish to acknowledge fruitful discussions with Jan Danckaert.

#82978 - $15.00 USD Received 11 May 2007; revised 31 Jul 2007; accepted 1 Aug 2007; published 24 Sep 2007
(C) 2007 OSA